

Is burn severity related to fire intensity? Observations from landscape scale remote sensing

Heather Heward^A, Alistair M. S. Smith^{A,D}, David P. Roy^B, Wade T. Tinkham^A, Chad M. Hoffman^C, Penelope Morgan^A and Karen O. Lannom^A

^ADepartment of Forest, Rangeland, and Fire Sciences, University of Idaho, Moscow, ID 83844, USA.

^BGeographic Information Science Center of Excellence, South Dakota State University, Brookings, SD 57007, USA.

^CDepartment of Forest and Rangeland Stewardship, Colorado State University, Fort Collins, CO 80523, USA.

^DCorresponding author. Email: alistair@uidaho.edu

Abstract. Biomass burning by wildland fires has significant ecological, social and economic impacts. Satellite remote sensing provides direct measurements of radiative energy released by the fire (i.e. fire intensity) and surrogate measures of ecological change due to the fire (i.e. fire or burn severity). Despite anecdotal observations causally linking fire intensity with severity, the nature of any relationship has not been examined over extended spatial scales. We compare fire intensities defined by Moderate Resolution Imaging Spectroradiometer Fire Radiative Power (MODIS FRP) products with Landsat-derived spectral burn severity indices for 16 fires across a vegetation structure continuum in the western United States. Per-pixel comparison of MODIS FRP data within individual fires with burn severity indices is not reliable because of known satellite temporal and spatial FRP undersampling. Across the fires, 69% of the variation in relative differenced normalized burn ratio was explained by the 90th percentile of MODIS FRP. Therefore, distributional MODIS FRP measures (median and 90th-percentile FRP) derived from multiple MODIS overpasses of the actively burning fire event may be used to predict potential long-term negative ecological effects for individual fires.

Received 2 June 2012, accepted 19 March 2013, published online 23 July 2013

Introduction

Biomass burning from wildland fires is a critical component of the Earth system and results in significant atmospheric, social, ecological and economic impacts; some immediate and several that last decades. Fires are also amongst the largest point source emitters of trace gas and aerosols to the atmosphere and are inherently variable in their timing, geographic extent and effects (Roy *et al.* 2008; Giglio *et al.* 2010; van der Werf *et al.* 2010). Fire continues to be a topic of public and policy concern in the United States; especially through the expansion of the wildland–urban interface where human–natural systems converge (Daniel *et al.* 2007; Paveglio *et al.* 2009). Despite intensive efforts at fire suppression, the western United States has experienced extensive fires in recent decades, with the area burned and occurrence of extreme fires expected to increase due to predicted changes in climate (Westerling *et al.* 2006; Littell *et al.* 2009). An improved understanding of these fires' characteristics and how social–ecological systems recover through time are required to provide land managers and policy makers with the information needed to prepare for, or mitigate, the effects of these events.

The burn severity of wildland fires can have significant effects on long-term (decadal) vegetation structure (Goetz *et al.* 2007), eco-hydrological processes (Adams *et al.* 2012)

and social systems (McCool *et al.* 2006). Definitions of severity vary, but is usually defined loosely as '*the magnitude of ecological change due to the fire*' (Lentile *et al.* 2006), or more quantitatively via metrics such as mortality of dominant vegetation, depth of litter and duff consumption, changes in species composition (Conard *et al.* 2002; Miller and Yool 2002). The term *fire severity* is often used to infer vegetation and soil changes that occur within the time frame of minutes to hours (Smith *et al.* 2005). In contrast, *burn severity* is often reserved for describing the effect of the fire over extended time frames of weeks to decades (Lentile *et al.* 2006; Keeley *et al.* 2008). Spatially explicit maps of burn severity, especially immediately following wildland fire events, are needed to assist land management planners in determining where to effectively allocate rehabilitation resources (Robichaud 2004). However, a complete understanding of the fire's severity may not be directly measureable until an extended period of time after fire occurrence. Fire severity is often estimated by visual or measured field observation of several ecological parameters (Key and Benson 2006) and burn severity is often inferred using multi-temporal (pre- and post-fire) airborne or satellite remotely sensed spectral indices (Lentile *et al.* 2006; Roy *et al.* 2006; French *et al.* 2008).

The term *fire intensity* refers to the rate of heat released during the fire and can be measured *in situ* using thermocouples and thermal cameras (Smith *et al.* 2005) or at extended spatial scales using airborne and satellite remotely sensed observations of the actively burning fire (Smith and Wooster 2005). Fire intensity and fire or burn severity have anecdotally been considered to be related, with more intense fires generally expected to cause more severe post-fire effects. To date, however, this has not been examined quantitatively at landscape scales over a large number of fires with varying fire behaviour. If satellite retrieved fire intensity and burn severity estimates are related then the relationship could provide new ways to predict potential areas of long-term negative ecological effects such as increases in tree mortality, worsening soil erosion or other extended post-fire effects (Lentile *et al.* 2006).

In this paper we aim to quantify and understand the relationship between satellite derived surrogates of burn severity and fire intensity using data at both Moderate Resolution Imaging Spectroradiometer Fire Radiative Power (MODIS FRP) pixel and per-fire extents. Satellite derived fire intensity measures (MODIS FRP data) are compared with burn severity estimates (as defined via Landsat spectral indices) for 16 fires across four broad vegetation types (herbaceous grassland, herbaceous shrub steppe, open tree canopy, closed tree canopy).

Background

Fire intensity

Conventionally the energy released during a fire has been characterised by fire line intensity (FLI, kW m^{-1}) measures that are a function of the heat released within the fuel that burned and the rate of spread of the fire front (Byram 1959). Byram's fire intensity model can be considered as the energy output from a strip of the actively combusting area, 1 m in length, that extends from the leading edge of the fire front to the rear of the flaming zone. Another similar measure of the energy released during a fire is the heat release rate per unit area (kW m^{-2}), also called the *fire reaction intensity* (Rothermel 1972). Fire reaction intensity is commonly used in several United States fire prediction systems (Ryan 2002; Sullivan 2009a; 2009b, 2009c). A third measure is the Fire Radiative Power (FRP, W) that describes the energy radiated by the fire per unit time, and may be retrieved at the locations of remotely sensed active fire detections from mid-infrared wavelength remotely sensed data (Kaufman *et al.* 1996). Laboratory studies of the FRP integrated over time have shown a strong linear relationship with the rate of fuel consumption (Wooster 2002; Freeborn *et al.* 2008; Kremens *et al.* 2010, 2012) supporting suppositions that FRP could be considered as a remote measure of the fire intensity (Wooster and Zhang 2004; Smith and Wooster 2005).

Burn severity

Burn severity is often assessed at landscape scales via remote sensing mapping methods and is commonly applied by land management agencies to describe post-fire effects under the broad terms of high, moderate and low burn severity (French *et al.* 2008). These broad qualitative descriptors are used to drive the identification of priority areas for post-fire rehabilitation

efforts to limit soil erosion, restore plant communities and prevent the establishment of invasive or noxious species (Robichaud 2009). Parameters used to estimate burn severity *in situ* include the condition and colour of the soil, the amount of fuel (duff, litter, surface and canopy fuels) consumed, resprouting from burned plants, consumption, mortality, blackening or scorching of trees and shrubs, depth of burn in the soil and changes in fuel moisture (Key and Benson 2006; Keeley *et al.* 2008; De Santis and Chuvieco 2009). Although several of these parameters are not amenable to optical wavelength remote sensing or may not be related in a linear way to reflectance (Royet *et al.* 2006; Disney *et al.* 2011); field-based estimates of burn severity (e.g. Composite Burn Index) are widely used to determine class breaks within the remote sensing products. The majority of these methods employ multi-temporal spectral indices (unitless) and most commonly the temporal differences in the normalised burn ratio (NBR) and variants thereof (Table 1; Lentile *et al.* 2006; French *et al.* 2008).

The normalised burn ratio was developed originally to detect burned areas, rather than to evaluate the variations within them (López Garcia and Caselles 1991) and past research has highlighted significant challenges with using this index for burn severity assessments (Roy *et al.* 2006; Smith *et al.* 2007; French *et al.* 2008; Lentile *et al.* 2009; Smith *et al.* 2010). However, other studies have shown reasonable empirical relationships ($R^2 = \sim 0.7$) between field-based tree mortality and multi-temporal changes in these indices (Keeley 2009; Lentile *et al.* 2009); especially in western United States ecosystems. As such, these relationships should only be considered appropriate for coarsely defined (high, moderate and low) burn severity classifications and are only reliably applicable where and when the relationships are calibrated with field data (French *et al.* 2008).

Linking fire intensity and burn severity

It is often remarked that fire intensity is correlated with fire or burn severity (Drewa 2003; Smith *et al.* 2005; Keeley 2009). This supposition is logical, as more intense fires are generally expected to have more significant post-fire effects and anecdotal observations support this. For example, high fire intensity crown fires tend to produce areas of high tree mortality, albeit in patches (Morgan *et al.* 2001). Higher intensity fires led to reduced resprouting of *Adenostoma fasciculatum* (Rosaceae) in chaparral systems (Borchert and Odion 1995) and similar responses

Table 1. Common metrics for inferring burn severity from satellite imagery

ρ_4 and ρ_7 are the top-of-atmosphere spectral reflectance as measured in bands 4 (0.76–0.90 μm) and 7 (2.08–2.35 μm) of the Landsat Enhanced Thematic Mapper (ETM+) sensor, NBR_i denotes pre-fire imagery and NBR_f denotes post-fire imagery

Spectral index	Equation	Reference
Normalised Burn Ratio	$\text{NBR} = (\rho_4 - \rho_7) \div (\rho_4 + \rho_7)$	Key and Benson (2006)
Differenced Normalised Burn Ratio	$\text{dNBR} = \text{NBR}_i - \text{NBR}_f$	Key and Benson (2006)
Relative Differenced Normalised Burn Ratio	$\text{RdNBR} = \text{dNBR} \div \sqrt{(\text{ABS}(\text{NBR}_i \div 1000))}$	Miller and Thode (2007)

are observed for African savanna brush species (Trollope and Tainton 1986). In contrast, grass species regrow even after very high intensity fires (Trollope and Tainton 1986), leading to studies characterising severity in terms of nitrogen fluxes within such systems (Smith *et al.* 2005). However, previous small area studies comparing metrics of fire intensity to fire effects observed few quantitative links (Ryan and Noste 1985; Hartford and Frandsen 1992; Smith *et al.* 2005), and others have observed that although the fire line intensity was ‘an indicator’ of some aboveground fire effects it was not sufficient to fully characterise the resultant effects on soil and vegetation (Alexander 1982; Hartford and Frandsen 1992). These prior observations covered a range of ecosystems including woodland and open African savannahs (Smith *et al.* 2005) to conifer dominated forests of the western United States (Ryan and Noste 1985; Hartford and Frandsen 1992).

Arguably, fire intensity and burn severity are two examples of a fire’s magnitude and are not necessarily related beyond observations that high values of each metric tend to occur concurrently (Ryan 2002). Moreover, satellite retrievals of fire intensity and burn severity are imperfect. The fire intensity retrieved from satellite data is sensitive to satellite temporal and spatial under-sampling due to infrequent satellite overpasses, cloud and smoke obscuration and failure to detect either cool or small fires (Boschetti and Roy 2009; Kumar *et al.* 2011) and satellite retrieved burn severity is dependent on the change in reflectance, the proportion of the satellite pixel that burned, the degree of combustion completeness and the reflectance of the pre-fire and unburned pixel components (Roy and Landmann 2005; Smith *et al.* 2005; Roy *et al.* 2010; Smith *et al.* 2010).

Methods

Sixteen fires that occurred in the summer months of 2005 and 2006 in the western United States were selected based on the availability of fire progression maps and ground truth

observations. The fires ranged from 400 to 50 000 ha in size (Fig. 1) and based on preliminary assessment of the fire data encompassed a wide range of burn severities and fire intensities. Daily fire perimeters were acquired from the United States National Interagency Fire Center (NIFC). The pre-fire vegetation cover for each fire was characterised using the 30-m LANDFIRE data 10 class nomenclature defined by the United States Geological Survey National Vegetation Classification System (NVCS). By overlaying the LANDFIRE data layers, pixels within each fire were then assigned to the classes: open tree canopy (25–60% canopy cover), closed tree canopy (60–100% canopy cover), herbaceous grassland or shrub steppe. Closed tree cover classes included only conifers whereas open included both conifers and hardwoods. Herbaceous grassland included grassland, exotic herbaceous and agricultural NVCS land cover classes.

Spectral indices used to define burn severity by the USGS were collated from the Monitoring Trends in Burn Severity (MTBS) project for each of the 16 fires (MTBS). As part of the MTBS protocol (Eidenshink *et al.* 2007), the Differenced Normalised Burn Ratio (dNBR) (Key and Benson 2006) and the relative version (RdNBR) developed for non-forested ecosystems (Miller and Thode 2007) are computed using 30-m spatial resolution Landsat imagery (Table 1). All Landsat 30-m pixels affected by clouds, cloud shadows and data gaps are discarded (Eidenshink *et al.* 2007).

The MTBS spectral indices are computed from Landsat data acquired as soon as possible (up to 16 days) after fire occurrence and ~1 year before in the same season, and under approximately similar phenological conditions (Eidenshink *et al.* 2007). The MTBS dNBR products are calculated with top-of-atmosphere (i.e. at sensor) reflectance that has not been corrected for atmospheric effects. If the atmosphere is variable this is a limitation of contemporary burn severity dNBR mapping assessments using multi-temporal imagery. However, atmospheric scattering in the Landsat 0.76–0.90- μm and 2.08–2.35- μm

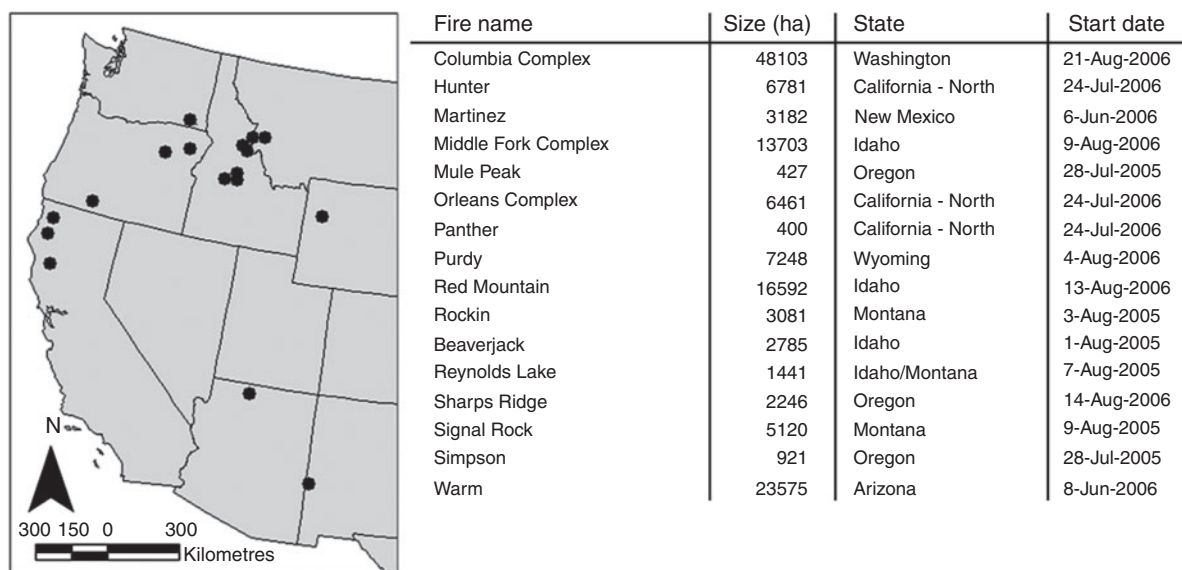


Fig. 1. Location, size and date of the 16 fires in the western United States.

wavelengths used to generate the NBR suite of indices is generally low, making atmospheric impacts less of a concern (Cocke *et al.* 2005; Ju *et al.* 2012).

The most recently available MODIS Collection 5 global monthly 1-km fire location product (MCD14ML) (Giglio 2010) that is derived from the MODIS active fire product (Giglio *et al.* 2003) was used. The product summarises the MODIS Terra (1030 and 2230 hours Equatorial overpass time) and MODIS Aqua (0130 and 1330 hours Equatorial overpass time) active fire detections providing, at the study area latitude, up to four detections and corresponding FRP estimates per day. In order to ensure correct spatial correspondence between the 30-m Landsat burn severity measures and the MODIS FRP data the relative geometry of the two sensor data were taken into account. The MODIS is a whiskbroom sensor with a 110° field of view (i.e. scan angles $\pm 55^\circ$) and so the MODIS active fire product detects fires that occur in pixels that increase in area from $\sim 1 \times 1$ km (at nadir) in the along-track direction 2×4.8 in the along-scan direction at scan edge respectively (Wolfe *et al.* 1998). The MODIS geolocation accuracy is 50 m (1σ) at nadir (Wolfe *et al.* 2002). Landsat sensors have a 15° field of view (i.e. scan angle $\pm 7.5^\circ$) and the change in pixel size as a function of scan angle is negligible and the Landsat geolocation accuracy is less than one 30-m pixel within the United States (Lee *et al.* 2004). A fire can occur anywhere within a MODIS pixel and its detection is dependent on several factors including the fire temperature and size, and the flaming fire front position relative to the along track MODIS triangular point spread function (Kaufman *et al.* 1998; Giglio 2010). Ichoku and Kaufman (2005) provide formulae for the MODIS pixel size as a function of scan angle and using them the MODIS pixel area is 50% greater than at nadir for scan angles greater than 27°. Consequently in this study: (i) only the MODIS FRP data for MODIS active fire detections with scan angles $\leq 27^\circ$ were used, (ii) a circular buffer with a radius of 0.5 km was placed around each of the remaining MODIS active fire detection pixel centre locations and (iii) only the MODIS active fire detections falling within each fire perimeter were considered. In this way we have confidence that only the 30-m dNBR and RdNBR burn severity values corresponding to the MODIS FRP data for the same fire events are compared.

Any part of the 0.5-km circular buffer that extended beyond the fire perimeter was clipped and not considered in the analysis. The MODIS FRP (MW) is derived using a nonlinear empirical relationship between the FRP and brightness temperature retrieved in the mid-infrared (Kaufman *et al.* 1998). The MODIS FRP is known to be sensitive to several factors including the presence of atmospheric water vapour, the fire background characterisation used in the FRP retrieval algorithm and the sub-pixel location of the fire and the sensing system point spread function (Wooster *et al.* 2005; Schroeder *et al.* 2010). All these factors introduce uncertainty into the subsequent analysis.

The mean dNBR and the mean RdNBR were calculated from all the 30-m Landsat pixels falling within the buffer region of each 1-km MODIS active fire detection. These mean burn severity values, which are co-located with active fire detections, were compared with the 1-km MODIS FRP (fire intensity values). A total of 1716 individual 1-km MODIS FRP values sensed across all 16 fires during the summer months of 2005 and

2006 were available with scan angle $\leq 27^\circ$. The two MODIS sensors usually have insufficient overpass frequency to provide MODIS FRP estimates that characterise the evolution of the fire behaviour at a fixed 1-km location and so the MODIS FRP values from multiple overpasses of the entire burned area or over many burned areas are derived (Roberts *et al.* 2009; Kumar *et al.* 2011).

In this paper distributional statistics (median, maximum and 90th-percentile) of the MODIS FRP values were derived for each of the 16 fires. The maximum MODIS FRP is of interest to researchers as the maximum fire intensity affects vegetation processes like grass and tree response to fire (Trollope and Tainton 1986; Archibald *et al.* 2010). The 90th-percentile MODIS FRP value was extracted to also capture this information as the maximum MODIS FRP value might only be associated with a singularly extreme fire behaviour event (such as blowups, rotating vertical plumes) that may only occupy a small spatial extent within the fire. Spatially, the fire might exhibit numerous patches of high fire intensity, which would not be captured by a maximum. Similarly, the median (the 50th-percentile) is of interest as a measure of the overall fire intensity within the fire.

The median, maximum and 90th-percentile MODIS FRP were compared with the mean of the 1-km RdNBR and to the mean of the 1-km dNBR burn severity estimates for all the pixels within each individual fire (Table 2). Fires with less than 10 samples were not included. These data were also analysed by four vegetation classes: herbaceous grassland, herbaceous shrub steppe, open tree canopy (25–60%) and closed tree canopy (60–100%). Insufficient individual fires were available in herbaceous cover classes ($n = 3$) to enable a reliable investigation. Linear and nonlinear regression models (logarithmic, power, cubic, quadratic, etc.) within the SPSS statistical package (Curve Estimation tool, Version 20, IBM Corp., New York) were used to find the model of best fit. All relationships were assessed at the 95th-confidence level. The coefficient of determination (R^2) and standard error of the estimate were used to evaluate different model fits.

Table 2. Significant relationships between metrics of burn severity (dNBR and RdNBR) and distributional metrics of fire radiative power (median and 90th percentile) overall and within two tree canopy closure percentage classes ($\alpha = 0.05$)

dNBR, differenced normalised burn ratio; RdNBR, relative differenced normalised burn ratio; FRP, fire radiative power. No significant relationships were found between burn severity metrics and maximum MODIS FRP

	Median FRP				90th Percentile FRP			
	R^2	n	F	s.e.m.	R^2	n	F	s.e.m.
dNBR								
Overall	–	–	–	–	–	–	–	–
25–60%	0.43 ^A	10	6.1	81	0.49 ^A	10	7.8	77
60–100%	–	–	–	–	–	–	–	–
RdNBR								
Overall	–	–	–	–	0.42 ^B	13	8.0	127
25–60%	0.63 ^A	10	13.6	135	0.69 ^A	10	18	122
60–100%	–	–	–	–	–	–	–	–

^ALinear relationship.

^BLogarithmic relationship.

Results and discussion

Fig. 2 shows scatter plots of mean 1-km RdNBR and dNBR against fire radiative power for all the 1-km MODIS pixels within all 16 fires. Both the RdNBR and dNBR are poorly related to the MODIS FRP at this scale. This is in part due to temporal sampling differences. Burn severity methods, collected either by satellite imagery methods such as RdNBR and dNBR or *in situ* (e.g. composite burn index), are principally measured following the fire. They integrate the effects that occurred before the fire, during the fire combustion phases and any post-fire processes into a single time-integrated measure. In contrast, fire intensity retrieved from MODIS FRP provides a temporally discrete measure at the time of satellite overpass, typically during the active combustion phase as detections require sufficient radiant energy to be released. These temporal samples are unlikely to capture the instances of maximum fire intensity as observed throughout the lifetime of the fire and typically high MODIS FRP values occur less frequently than low MODIS FRP values (Kumar *et al.* 2011). In addition, these differences may be due to the different spatial resolution of the MODIS active fire detections (nominally 1 km at nadir) and the 30-m spatial resolution of Landsat, as aggregation of the 30-m pixels to the 1-km scale will reduce variability.

The data illustrated in Fig. 2 indicate that the variation in the mean burn severity metrics decreases with greater MODIS FRP. This pattern was found for the four vegetation cover classes and for individual fires (Fig. 3). Similar patterns with *in situ* field metrics of burn severity and fire intensity have been observed in past studies (Smith *et al.* 2005). These results are somewhat expected as low intensity fires generally result in a wide range of spatially heterogeneous ecological effects (pockets of white ash, mortality, light char, unburned, etc.); whereas high intensity fires often lead to more spatially homogenous effects across contiguous areas of the fire (vegetation mortality, exposure of mineral soil, etc.) (Lentile *et al.* 2006). We recognise that this could also be associated with errors in the MODIS FRP which can be underestimated depending on the sub-pixel location of the active fire with respect to the central-pixel location (Schroeder *et al.* 2010), the presence of atmospheric water vapor (Wooster *et al.* 2005) and because at high MODIS scan angles only larger and hotter actively burning fires tend to be detected (Giglio *et al.* 1999; Freeborn *et al.* 2011) and they tend to have lower FRP (Kumar *et al.* 2011).

Table 2 summarises relationships between both dNBR and RdNBR with the 90th-percentile and median MODIS FRP for all fires and within tree canopy cover classes. The underlying assumption of these comparisons is that the distributional statistics for each of the fires captures the prevailing fire behaviour and ecological effects. No significant relationships were found between the burn severity metrics and maximum MODIS FRP and so these results are not tabulated. This indicates that singularly observed high values of MODIS FRP, such as may arise from extreme fire behaviour, are not indicative of the overall fire behaviour and effects; although this could also be because at the time of satellite overpass the fire was not burning with maximum fire intensity and the peaks were under-sampled (Kumar *et al.* 2011). Overall, MODIS FRP was a better

predictor of RdNBR than dNBR (Table 2). RdNBR was designed to capture the relative change in biomass whereas MODIS FRP provides a measure of the quantity of fuel combusted (Kaufman *et al.* 1996). In contrast, dNBR provides an estimate of the relative change in vegetation and soil or char cover (Lentile *et al.* 2009; Smith *et al.* 2010).

Fig. 4 shows that within the two tree cover classes the median and 90th-percentile MODIS FRP per fire are reasonable predictors of RdNBR whereas across all cover classes the 90th-percentile MODIS FRP is a reasonable predictor. In each case an asymptote is observed in the RdNBR values indicating a lack of index sensitivity at higher fire intensities. This asymptote has also been observed in numerous field studies (Cocke *et al.* 2005; French *et al.* 2008). Across the fires, 69% of the variation in RdNBR was explained by the 90th-percentile of MODIS FRP (Table 2, Fig. 4). Thus, misrepresentation of predicted burn severity due to satellite MODIS FRP sampling issues may potentially be overcome by use of MODIS FRP distributional statistics.

These results highlight further challenges beyond those already described with the usage of dNBR and RdNBR to assess post-fire effects at landscape scales. The rapid asymptote of

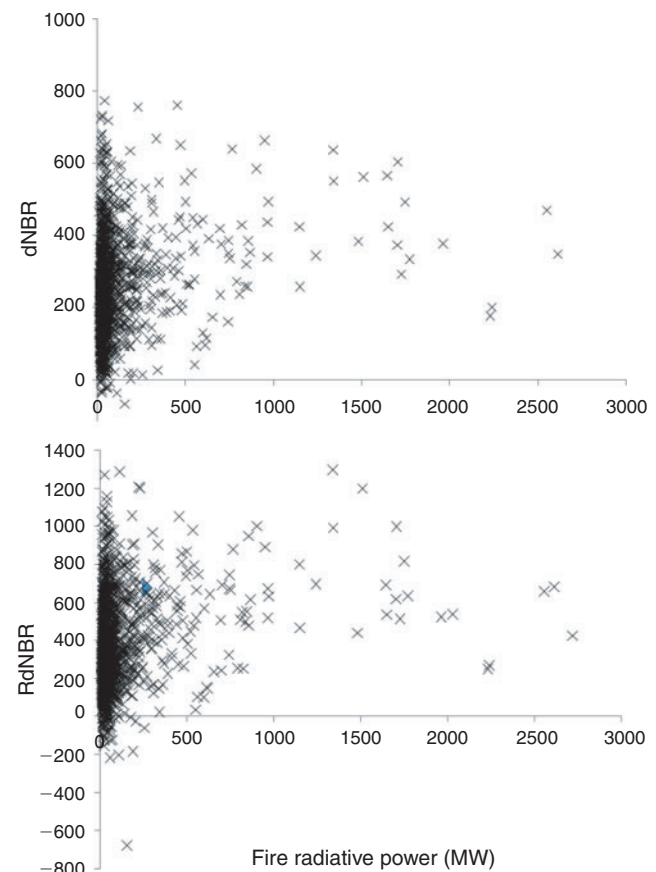


Fig. 2. Scatterplots of mean differenced normalised burn ratio (dNBR) and relative differenced normalised burn ratio (RdNBR) with co-located 1-km MODIS fire radiative power (MW) observations for data from all 16 fires ($n = 1716$).

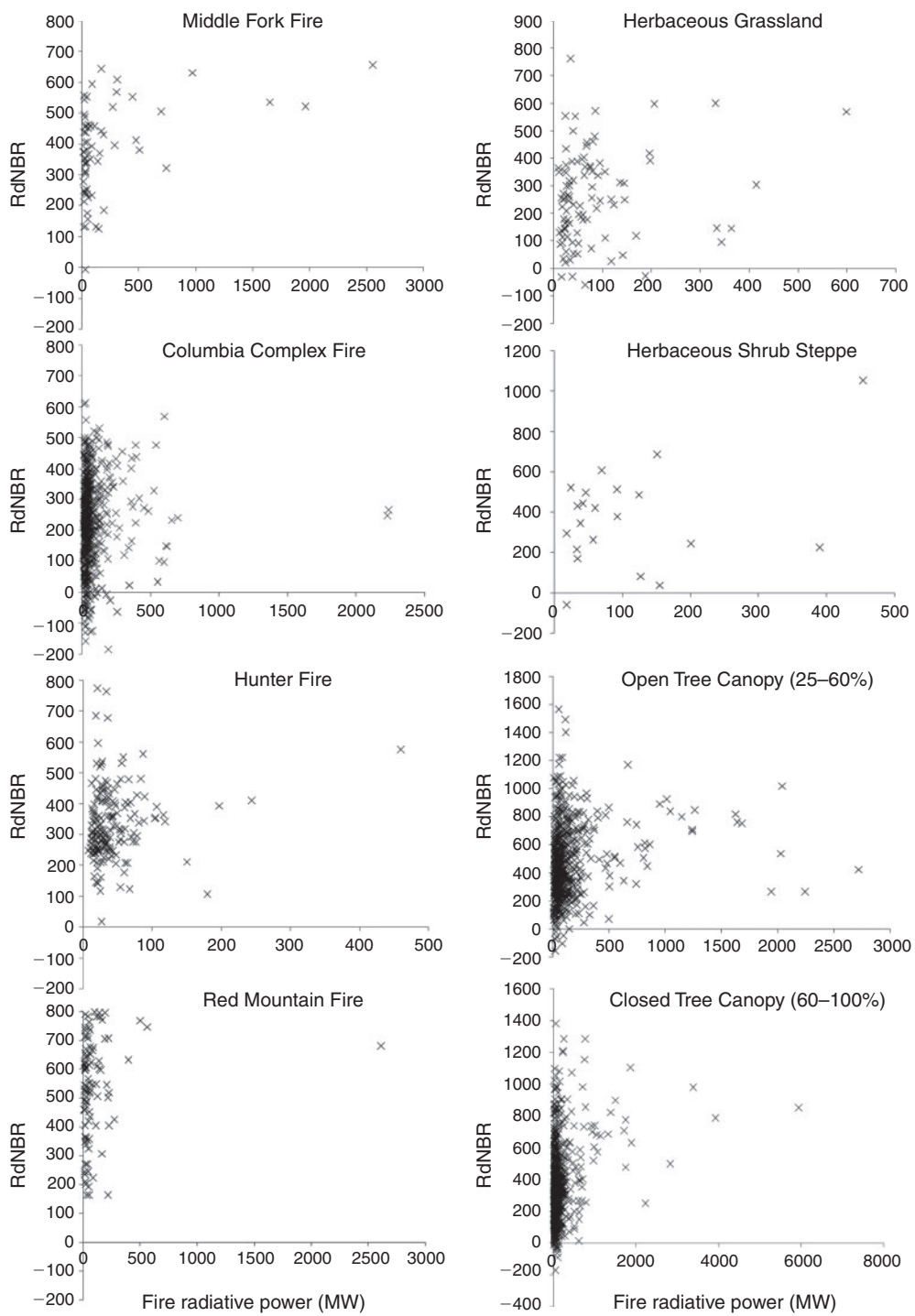


Fig. 3. Scatterplots of mean relative differenced normalised burn ratio (RdNBR) with 1-km MODIS fire radiative power (MW) observations for data from four of the fires (Middle Fork fire, $n = 71$; Columbia complex fire, $n = 642$; Hunter fire, $n = 178$; Red Mountain fire, $n = 125$) and across four vegetation types (Herbaceous grassland, $n = 95$; Herbaceous shrub steppe, $n = 21$; Open Tree Canopy, $n = 606$; Closed Tree Canopy, $n = 904$). The twelve remaining fires assessed showed similar patterns.

RdNBR at FRP values lower than one-third of the data range highlights the general insensitivity of this burn severity index to fire intensity. This observed insensitivity and the broad limitations in the dNBR family of spectral indices that have

been discussed suggest that they should only be linked to specific post-fire effects at each fire location (e.g. tree mortality) and then subsequent discussions should only describe trends in that effect (e.g. Miller *et al.* 2008).

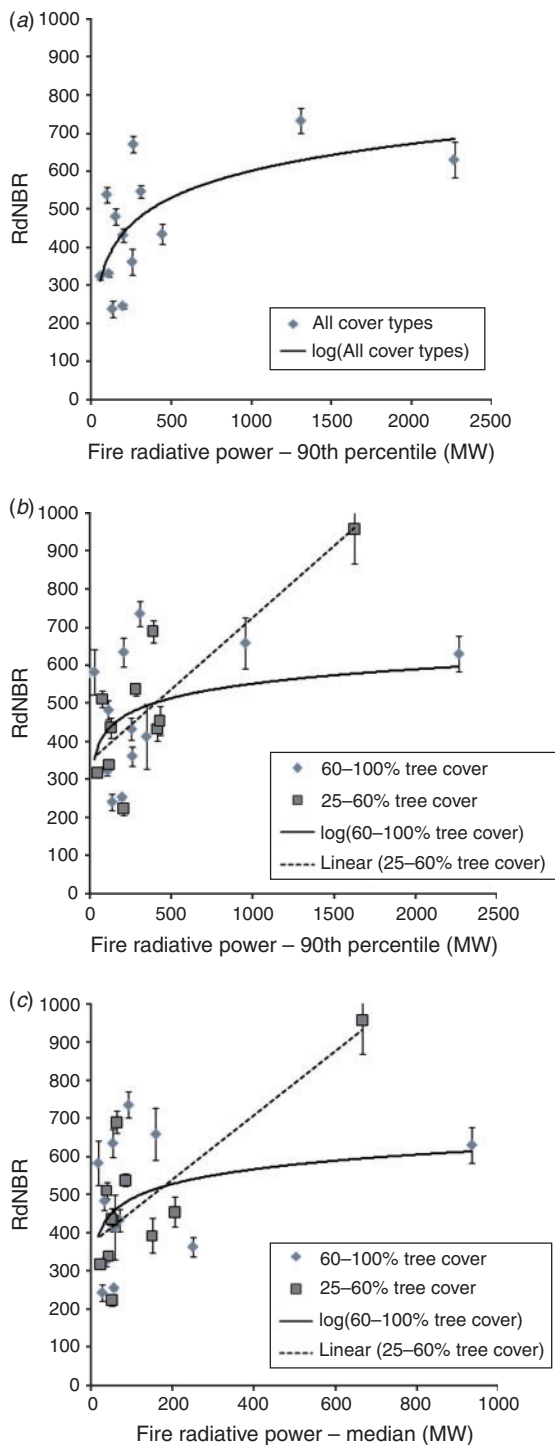


Fig. 4. Mean Landsat derived RdNBR for each fire (error bars show standard error of the mean) plotted against metrics of MODIS 1-km FRP (MW) for all active fire detections. MODIS FRP metrics plotted are (a) 90th percentile MODIS FRP for all fires with greater than 10 samples ($n = 13$), (b) 90th percentile MODIS FRP for each fire stratified by high (60–100%, $n = 13$) and moderate (25–60%, $n = 10$) tree cover class types, (c) Median MODIS FRP for each fire stratified by high (60–100%, $n = 13$) and moderate (25–60%, $n = 10$) tree cover class types. Insufficient MODIS FRP points or individual fires were available in low tree cover classes (<25%, $n = 3$) to enable a rigorous investigation.

Conclusions

Distributional measures of MODIS FRP have potential to be used to predict potential high severity and long-term negative ecological effects (as indicated by RdNBR in this case) when applied at the extended spatial–temporal scales of individual wildland fire events. Overall, MODIS FRP was a better predictor of RdNBR than dNBR, potentially indicating a closer mechanistic link. To avoid MODIS FRP temporal and spatial under-sampling (Boschetti and Roy 2009; Kumar *et al.* 2011) this work illustrates that MODIS FRP data should not be evaluated on a 1-km pixel scale to relate to Landsat-derived RdNBR or dNBR. In other regions, especially at high boreal latitudes where MODIS overpasses many times per day and where fires can burn for many days this may not be the case. MODIS is used in regional, national and global assessments of fire occurrence and extent. As a result, the MODIS FRP distributional statistics could provide continental scale predictions of burn severity per fire. Such information could potentially be used within national fire management budget planning programs, such as Fire Program Analysis (FPA) used within the United States, to help predict post-fire recovery and rehabilitation costs. In order to understand the fine scale variability of fire intensity it may be worth investigating the spatial distribution of burn severity metrics within individual MODIS FRP pixels. To overcome the spatial and temporal integration challenges of comparing burn severity to fire intensity, field research is also warranted to coincidentally measure *in situ* active fire behaviour with prior fuels and post-fire ecological effects. Further research is needed to develop new severity indices that exhibit greater sensitivity as a function of fire behaviour and ecological (and spectral) change.

Acknowledgements

Heather Heward, Alistair M. S. Smith and David P. Roy contributed equally to this work. This work was partially supported by the NSF Idaho EPSCoR Program and by the National Science Foundation under award number EPS-0814387. Partial funding support was received via Joint Fire Sciences Program under award number 07–2–1–60 and the National Aeronautics and Space Administration (NASA) under award NNX11AO24G. We also recognise NASA and USGS for providing the satellite imagery. A special thanks to Louis Giglio for his assistance with the usage of the MODIS data products.

References

- Adams HD, Luce CD, Breshears DD, Allen CD, Weiler M, Hale VC, Smith AMS, Huxman TE (2012) Ecohydrological consequences of drought- and infestation-triggered tree die-off: insights and hypotheses. *Ecohydrology* **5**(2), 145–159. doi:10.1002/ECO.233
- Alexander ME (1982) Calculating and interpreting forest fire intensities. *Canadian Journal of Botany* **60**(4), 349–357. doi:10.1139/B82-048
- Archibald S, Scholes RJ, Roy DP, Roberts G, Boschetti L (2010) Southern African fire regimes as revealed by remote sensing. *International Journal of Wildland Fire* **19**(7), 861–878. doi:10.1071/WF10008
- Borchert MI, Odion DC (1995) Fire intensity and vegetation recovery in chaparral: a review. In 'Bushfire in California Wildlands: Ecology and Resource Management'. (Eds JE Keeley, T Scott) pp. 91–100. (International Association of Wildland Fire: Fairfield, WA)
- Boschetti L, Roy DP (2009) Strategies for the fusion of satellite fire radiative power with burned area data for fire radiative energy derivation. *Journal of Geophysical Research* **114**, D20302. doi:10.1029/2008JD011645

- Byram GM (1959) Combustion of forest fuels. In 'Fire: Control and Use'. (Ed. KP Davis) pp. 61–89. (McGraw Hill: New York)
- Cocke AE, Fule PZ, Crouse JE (2005) Comparison of burn severity assessments using Differenced Normalized Burn Ratio and ground data. *International Journal of Wildland Fire* **14**(2), 189–198. doi:10.1071/WF04010
- Conard SG, Sukhinin AI, Stocks BJ, Cahoon DR, Davidenko EP, Ivanova GA (2002) Determining effects of area burned and fire severity on carbon cycling and emissions in Siberia. *Climatic Change* **55**, 197–211. doi:10.1023/A:1020207710195
- Daniel TC, Carroll MS, Moseley C, Raish C (Eds) (2007) 'People, Fire and Forests: a Synthesis of Wildfire Social Science'. (Oregon State University Press: Corvallis, OR)
- De Santis A, Chuvieco E (2009) GeoCBI: a modified version of the Composite Burn Index for the initial assessment of the short-term burn severity from remotely sensed data. *Remote Sensing of Environment* **113**(3), 554–562. doi:10.1016/J.RSE.2008.10.011
- Disney MI, Lewis P, Gomez-Dans J, Roy D, Wooster MJ, Lajas D (2011) 3D radiative transfer modelling of fire impacts on a two-layer savanna system. *Remote Sensing of Environment* **115**(8), 1866–1881. doi:10.1016/J.RSE.2011.03.010
- Drewa PB (2003) Effects of fire season and intensity on *Prosopis glandulosa* Torr. var. *glandulosa*. *International Journal of Wildland Fire* **12**(2), 147–157. doi:10.1071/WF02021
- Eidsenink J, Schwind B, Brewer K, Zhu Z, Quayle B, Howard S (2007) A project for monitoring trends in burn severity. *Journal of Fire Ecology* **3**(1), 3–21. doi:10.4996/FIRECOLOGY.0301003
- Freeborn PH, Wooster MJ, Min Hao W, Ryan CA, Nordgren BL, Baker AP, Ichoku C (2008) Relationships between energy release, fuel mass loss, and trace gas and aerosol emissions during laboratory biomass fires *Journal of Geophysical Research* **113**, D01301. doi:10.1029/2007JD008679
- Freeborn PH, Wooster MJ, Roberts G (2011) Addressing the spatiotemporal sampling design of MODIS to provide estimates of the fire radiative energy emitted from Africa. *Remote Sensing of Environment* **115**(2), 475–489. doi:10.1016/J.RSE.2010.09.017
- French NHF, Kasischke ES, Hall RJ, Murphy KA, Verbyla DL, Hoy EE, Allen JL (2008) Using Landsat data to assess fire and burn severity in the North American boreal forest region: an overview and summary of results. *International Journal of Wildland Fire* **17**(4), 443–462. doi:10.1071/WF08007
- Giglio L (2010) 'MODIS Collection 5 Active Fire product User's Guide Version 2.4'. (University of Maryland: College Park, MD)
- Giglio L, Kendall JD, Justice CO (1999) Evaluation of global fire detection algorithms using simulated AVHRR infrared data. *International Journal of Remote Sensing* **20**(10), 1947–1985. doi:10.1080/014311699212290
- Giglio L, Descloitres J, Justice CO, Kaufman YJ (2003) An enhanced contextual fire detection algorithm for MODIS. *Remote Sensing of Environment* **87**(2–3), 273–282. doi:10.1016/S0034-4257(03)00184-6
- Giglio L, Randerson JT, van der Werf GR, Kasibhatla PS, Collatz GJ, Morton DC, DeFries RS (2010) Assessing variability and long-term trends in burned area by merging multiple satellite fire products. *Biogeosciences* **7**, 1171–1186. doi:10.5194/BG-7-1171-2010
- Goetz SJ, Mack MC, Gurney KR, Randerson JT, Houghton RA (2007) Ecosystem responses to recent climate change and fire disturbance at northern high latitudes: observations and model results contrasting northern Eurasia and North America. *Environmental Research Letters* **2**(4), 045031. doi:10.1088/1748-9326/2/4/045031
- Hartford RA, Frandsen WH (1992) When it's hot, it's hot- or maybe it's not! (Surface flaming may not portend extensive soil heating) *International Journal of Wildland Fire* **2**(3), 139–144. doi:10.1071/WF920139
- Ichoku C, Kaufman YK (2005) A method to derive smoke emission rates from MODIS fire radiative energy measurements. *IEEE Transactions on Geoscience and Remote Sensing* **43**(11), 2636–2649. doi:10.1109/TGRS.2005.857328
- Ju J, Roy DP, Vermote E, Masek J, Kovalskyy V (2012) Continental-scale validation of MODIS-based and LEDAPS Landsat ETM+ atmospheric correction methods. *Remote Sensing of Environment* **122**, 175–184. doi:10.1016/J.RSE.2011.12.025
- Kaufman YJ, Remer LA, Ottmar RD, Ward DE, Li RR, Kleidman R, Fraser RA, Flynn L, McDougal D, Shelton G (1996) Relationship between remotely sensed fire intensity and rate of emission of smoke: SCAR-C experiment. In 'Global Biomass Burning'. (Ed. JS Levine) pp. 685–696. (MIT Press: Cambridge, MA)
- Kaufman YJ, Justice CO, Flynn LP, Kendall JD, Prins EM, Giglio L, Ward DE, Menzel WP, Setzer AW (1998) Potential global fire monitoring from EOS-MODIS. *Journal of Geophysical Research* **103**(D24), 32215–32238. doi:10.1029/98JD01644
- Keeley JE (2009) Fire intensity, fire severity and burn severity: a brief review and suggested usage. *International Journal of Wildland Fire* **18**(1), 116–126. doi:10.1071/WF07049
- Keeley JE, Brennan T, Pfaff AH (2008) Fire severity and ecosystem responses following crown fires in California shrublands. *Ecological Applications* **18**, 1530–1546. doi:10.1890/07-0836.1
- Key CH, Benson NC (2006) Landscape assessment: Ground measure of severity, the Composite Burn Index; and remote sensing of severity, the Normalized Burn Ratio. In 'FIREMON: Fire Effects Monitoring and Inventory System'. (Eds. DC Lutes, RE Keane, JF Caratti, CH Key, NC Benson, S Sutherland, LJ Gangi) USDA Forest Service, Rocky Mountain Research Station, General Technical Report RMRS-GTR-164-CD: LA, pp. 1–51. (Ogden, UT)
- Kremens RL, Smith AMS, Dickinson MB (2010) Fire metrology: current and future directions in physics-based measurements. *Fire Ecology* **6**(1), 13–35. doi:10.4996/FIRECOLOGY.0601013
- Kremens RL, Dickinson MB, Bova AS (2012) Radiant flux density, energy density and fuel consumption in mixed-oak forest surface fires. *International Journal of Wildland Fire* **21**(6), 722–730. doi:10.1071/WF10143
- Kumar SS, Roy DP, Boschetti L, Kremens R (2011) Exploiting the power law distribution properties of satellite fire radiative power retrievals – a method to estimate fire radiative energy and biomass burned from sparse satellite observations. *Journal of Geophysical Research* **116**, D19303. doi:10.1029/2011JD015676
- Lee DS, Storey JC, Choate MJ, Hayes R (2004) Four years of Landsat-7 on-orbit geometric calibration and performance. *IEEE Transactions on Geoscience and Remote Sensing* **42**, 2786–2795. doi:10.1109/TGRS.2004.836769
- Lentile LB, Holden ZA, Smith AMS, Falkowski MJ, Hudak AT, Morgan P, Lewis SA, Gessler PE, Benson NC (2006) Remote sensing techniques to assess active fire and post-fire effects. *International Journal of Wildland Fire* **15**(3), 319–345. doi:10.1071/WF05097
- Lentile LB, Smith AMS, Hudak AT, Morgan P, Bobbitt MJ, Lewis SA, Robichaud PR (2009) Remote sensing for prediction of 1-year post-fire ecosystem condition. *International Journal of Wildland Fire* **18**(5), 594–608. doi:10.1071/WF07091
- Littell JS, McKenzie D, Peterson DL, Westerling AL (2009) Climatic influences on twentieth-century area burned in ecoprovinces of the western U.S. *Ecological Applications* **19**(4), 1003–1021. doi:10.1890/07-1183.1
- López García MJ, Caselles V (1991) Mapping burns and natural reforestation using Thematic Mapper data. *Geocarto International* **6**(1), 31–37. doi:10.1080/10106049109354290
- McCool SF, Burchfield JA, Carroll MS (2006) An event-based approach for examining the effects of wildland fire decisions on communities. *Environmental Management* **37**(4), 437–450. doi:10.1007/S00267-005-0054-0
- Miller JD, Thode AE (2007) Quantifying burn severity in a heterogeneous landscape with a relative version of the delta Normalized Burn Ratio

- (dNBR). *Remote Sensing of Environment* **109**(1), 66–80. doi:10.1016/J.RSE.2006.12.006
- Miller JD, Yool SR (2002) Mapping forest post-fire canopy consumption in several overstory types using multi-temporal Landsat TM and ETM data. *Remote Sensing of Environment* **82**, 481–496. doi:10.1016/S0034-4257(02)00071-8
- Miller JD, Safford HD, Crimmins M, Thode AE (2008) Quantitative evidence for increasing forest fire severity in the Sierra Nevada and Southern Cascade Mountains, California and Nevada, USA *Ecosystems*. doi:10.1007/S10021-008-9201-9
- Morgan P, Hardy CC, Swetnam TW, Rollins MG, Long DG (2001) Mapping fire regimes across time and space: understanding coarse and fine-scale fire patterns. *International Journal of Wildland Fire* **10**(4), 329–342. doi:10.1071/WF01032
- Paveglio TB, Jakes PJ, Carroll MS, Williams DR (2009) Understanding social complexity within the wildland–urban interface: a new species of human habitation? *Environmental Management* **43**(6), 1085–1095. doi:10.1007/S00267-009-9282-Z
- Roberts G, Wooster MJ, Lagoudakis E (2009) Annual and diurnal African biomass burning temporal dynamics. *Biogeosciences* **6**(5), 849–866. doi:10.5194/BG-6-849-2009
- Robichaud PR (2004) Postfire rehabilitation treatments: are we learning what works? *Southwest Hyrdology* **5**, 20–21.
- Robichaud PR (2009) Post-fire Stabilization and Rehabilitation. In ‘Fire Effects on Soils and Restoration Strategies’. (Eds A. Cerda and P. R. Robichaud.) pp. 299–320. (Science Publishers: Enfield, NH)
- Rothermel RC (1972) A mathematical model for predicting fire spread in wildland fuels. USDA Forest Service, Research Paper INT-115. (Ogden, UT)
- Roy DP, Landmann T (2005) Characterizing the surface heterogeneity of fire effects using multi-temporal reflective wavelength data. *International Journal of Remote Sensing* **26**(19), 4197–4218. doi:10.1080/01431160500112783
- Roy DP, Boschetti L, Trigg S (2006) Remote sensing of fire severity: assessing the performance of the normalized burn ratio. *IEEE Geoscience and Remote Sensing Letters* **3**(1), 112–116. doi:10.1109/LGRS.2005.858485
- Roy DP, Boschetti L, Justice CO, Ju J (2008) The collection 5 MODIS burned area product – global evaluation by comparison with the MODIS active fire product. *Remote Sensing of Environment* **112**(9), 3690–3707. doi:10.1016/J.RSE.2008.05.013
- Roy DP, Boschetti L, Maier SW, Smith AMS (2010) Field estimation of ash and char colour-lightness using a standard gray scale. *International Journal of Wildland Fire* **19**(6), 698–704. doi:10.1071/WF09133
- Ryan KC (2002) Dynamic interactions between forest structure and fire behavior in boreal ecosystems. *Silva Fennica* **36**(1), 13–39.
- Ryan KC, Noste NV (1985) Evaluating prescribed fires. In ‘Proceedings of the symposium and workshop on wilderness fire’, 15–18 November 1983, Missoula, MT. (Eds. JE Lotan, BM Kilgore, WC Fischer, RW Mutch) USDA Forest Service, Intermountain Forest and Range Experiment Station, General Technical Report INT-GTR-182, pp. 230–238. (Ogden, UT)
- Schroeder W, Csizsar I, Giglio L, Schmidt CC (2010) On the use of fire radiative power, area, and temperature estimates to characterize biomass burning via moderate to coarse spatial resolution remote sensing data in the Brazilian Amazon. *Journal of Geophysical Research* **115**(D21), D21121. doi:10.1029/2009JD013769
- Smith AMS, Wooster MJ (2005) Remote classification of head and backfire types from MODIS fire radiative power and smoke plume observations. *International Journal of Wildland Fire* **14**(3), 249–254. doi:10.1071/WF05012
- Smith AMS, Wooster MJ, Drake NA, Dipotso FM, Falkowski MJ, Hudak AT (2005) Testing the potential of multi-spectral remote sensing for retrospectively estimating fire severity in African Savannas. *Remote Sensing of Environment* **97**(1), 92–115. doi:10.1016/J.RSE.2005.04.014
- Smith AMS, Lentile LB, Hudak AT, Morgan P (2007) Evaluation of linear spectral unmixing and dNBR for predicting post-fire recovery in a North American ponderosa pine forest. *International Journal of Remote Sensing* **28**(22), 5159–5166. doi:10.1080/01431160701395161
- Smith AMS, Eitel JUH, Hudak AT (2010) Spectral analysis of charcoal on soils: implications for wildland fire severity mapping methods. *International Journal of Wildland Fire* **19**, 976–983. doi:10.1071/WF09057
- Sullivan AL (2009a) Wildland surface fire spread modelling, 1990–2007. 1. Physical and quasi-physical models. *International Journal of Wildland Fire* **18**(4), 349–368. doi:10.1071/WF06143
- Sullivan AL (2009b) Wildland surface fire spread modelling, 1990–2007. 2. Empirical and quasi-empirical models. *International Journal of Wildland Fire* **18**(4), 369–386. doi:10.1071/WF06142
- Sullivan AL (2009c) Wildland surface fire spread modelling, 1990–2007. 3. Simulation and mathematical analogue models. *International Journal of Wildland Fire* **18**(4), 387–403. doi:10.1071/WF06144
- Trollope WSW, Tainton NM (1986) Effect of fire intensity on the grass and bush components of the Eastern Cape thornveld. *African Journal of Range and Forage Science* **3**, 37–42.
- van der Werf GR, Randerson JT, Giglio L, Collatz GJ, Mu M, Kasibhatla PS, Morton DS, DeFries RS, Jin Y, van Leeuwen TT (2010) Global fire emissions and the contribution of deforestation, savanna, forest, agricultural, and peat fires (1997–2009) *Atmospheric Chemistry and Physics Discussion* **10**, 16153–16230. doi:10.5194/ACPD-10-16153-2010
- Westerling AL, Hidalgo HG, Cayan DR, Swetnam TW (2006) Warming and earlier spring increase western US forest wildfire activity. *Science* **313**(5789), 940–943. doi:10.1126/SCIENCE.1128834
- Wolfe RE, Roy DP, Vermote E (1998) MODIS land data storage, gridding, and compositing methodology: level 2 grid, Geoscience and Remote Sensing. *IEEE Transactions on Geoscience and Remote Sensing* **36**(4), 1324–1338. doi:10.1109/36.701082
- Wolfe RE, Nishihama M, Fleig A, Kuyper J, Roy DP, Storey J, Patt F (2002) Achieving sub-pixel geolocation accuracy in support of MODIS land science. *Remote Sensing of Environment* **83**, 31–49. doi:10.1016/S0034-4257(02)00085-8
- Wooster MJ (2002) Small-scale experimental testing of fire radiative energy for quantifying mass combusted in natural vegetation fires. *Geophysical Research Letters* **29**(21), 2027. doi:10.1029/2002GL015487
- Wooster MJ, Zhang YH (2004) Boreal forest fires burn less intensely in Russia than in North America. *Geophysical Research Letters* **31**, L20505. doi:10.1029/2004GL020805
- Wooster MJ, Roberts G, Perry GLW, Kaufman YJ (2005) Retrieval of biomass combustion rates and totals from fire radiative power observations: FRP derivation and calibration relationships between biomass consumption and fire radiative energy release. *Journal of Geophysical Research* **110**(D24), D24311. doi:10.1029/2005JD006318